

ADC of Prostate Tissue *In vivo* at 3T

R. Bourne¹, P. Stanwell¹, S. Ramadan¹, P. Katelaris¹, C. Mountford¹

¹Department of Magnetic Resonance in Medicine, University of Sydney, Institute for Magnetic Resonance Research, Sydney, NSW, Australia

Introduction: Apparent diffusion coefficient (ADC) measured by MR reflects physical properties of tissue that correlate with the microscopic architectural structure seen by histopathology (1). Measurements of prostate tissue ADC from in-vivo 1.5T diffusion-weighted MR imaging (DWI) have provided only weak discrimination between malignant and benign tissue even within the predominantly glandular peripheral zone (2-3). Here we have used EPI-based DWI method to measure prostate tissue ADC at the higher field strength of 3T.

Methods: Thirty three patients were examined prior to TRUS biopsy or radical prostatectomy. MR imaging was performed on a clinical 3T whole body scanner (Magnetom Trio, Siemens AG, Germany) using disposable endorectal coils (Innervue, Medrad, USA). Axial, coronal, and sagittal FSE T2-weighted images (TR/TE 4000/130ms), and axial T1-weighted images (TR/TE 500/22ms) were acquired. The field of view (FOV) for T2 and T1 images was 15x15cm. Axial diffusion-weighted imaging was undertaken using a single-shot echo planar imaging sequence (EPI) with four incremented b-values ($b = 0, 150, 300, 400 \text{ sec.mm}^{-2}$) in three orthogonal planes (FOV=22x8 cm, matrix = 128x45). Slices were placed coplanar with axial T2-weighted slices. Average ADC values were calculated from the three orthogonal ADC values. Voxels for measurement of ADC were selected on the basis of T2 and DWI imaging characteristics. Correlative histopathology was obtained either at TRUS biopsy or after radical prostatectomy. Voxels representative of malignant tissue were selected from regions of low T2 and DW intensity where a positive TRUS biopsy was obtained from the immediate vicinity. Voxels representative of benign tissue were selected from regions of high T2 and DW intensity where no positive TRUS biopsy was obtained from the vicinity. Stromal nodule voxels were selected as well-defined circular central gland regions of low T2 and DW intensity where no positive TRUS biopsy was obtained from the vicinity. Glandular nodule voxels were selected from well-defined circular central gland regions of high T2 and DW intensity where no positive TRUS biopsy was obtained from the vicinity. Normal (benign) central gland was selected from patients with no DWI, T2, or biopsy indication of central gland cancer.

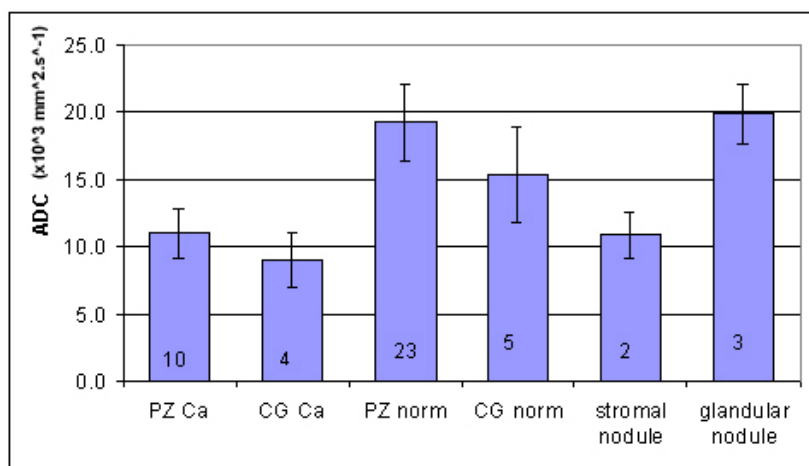


Figure 1: Average ADC measured at 3T in prostate tissue. Error bars represent \pm SD. Numbers at the bottom of each column represent number of voxels measured (PZ: peripheral zone, CZ: central and transition zone, Ca: adenocarcinoma, norm: benign).

Results and Discussion: A comparison of ADC values measured in different prostate tissue types is shown in Fig. 1. It can be seen that there is a clear distinction between the cancer and normal tissue for both peripheral and central zones. Although the measured ADC of central gland cancer was similar to the ADC of stromal nodules commonly found in patients with BPH, central gland adenocarcinoma can usually be distinguished from stromal nodules in T2 images by its ill-defined boundaries and stippled texture. In contrast, stromal nodules typically have a well-defined circular shape and are homogeneously hypointense in T2 images. Previously 1.5T measurements of prostate tissue ADC have suggested only weak discrimination between malignant and benign tissue even within the predominantly glandular peripheral zone (1-3). The improved discrimination observed at 3T compared with 1.5T may be partially due to the higher SNR available at 3T, but also to the more strict imaging and histopathology criteria applied here to the selection of voxels.

Conclusions: This is the first report of prostate tissue ADC measured at 3T. Calculation of prostate tissue ADC from DWI at 3T improves T2-based discrimination between benign and malignant tissue in both the central and peripheral zones of the prostate.

References

1. Anderson A. et al. MRI 18:689-695 (2000)
2. Sato C. et al. JMRI 21:258-262 (2005)
3. Issa B. JMRI 16: 196-200 (2002)
4. Gibbs P. et al., MRM 46:1054-1058 (2001)